New Limits on Local Lorentz Invariance from Hg and Cs Magnetometers

C. J. Berglund, L. R. Hunter, D. Krause, Jr., E. O. Prigge, and M. S. Ronfeldt
Physics Department, Amherst College, Amherst, Massachusetts 01002

S. K. Lamoreaux
Physics Department, University of Washington, Seattle, Washington 98195
(Received 15 May 1995)

The relative frequency of Hg and Cs mgnetometers is monitored as a function of the orientation of the applied magnetic field with respect to the fixed stars. The observed stability of the relative frequency limits electron and nucleon local Lorentz invariance violating effects to less than 200 μHz and 110 nHz, respectively. These results represent an improvement over the best published results by an order of magnitude for electron effects and by a factor of 240 for nuclear effects. The result also sets an upper limit of 200 eV on the Fermi level of a degenerate remnant neutrino background.

PACS numbers: 03.30.+p, 07.57.Pt, 11.30.Cp, 32.80.Bx

All metric theories of gravity are based upon the Einstein equivalence principle which assumes both the weak equivalence principle and local Lorentz invariance (LLI). The LLI postulate states that the outcome of any local nongravitational experiment is independent of the velocity and orientation of the freely falling apparatus. This postulate has been well tested for electromagnetism by the classic experiments of Michelson and Morley [1] and by modern descendants of those experiments [2]. Nielson and Picek have explored the experimental consequences of a preferred metric for the weak interaction and have concluded that by far the most sensitive limits on such a preferred frame are produced by the measurement of a Hamiltonian of the form $H = Kh\boldsymbol{\sigma} \cdot \mathbf{p}$, where $\boldsymbol{\sigma}$ is a unit vector in the direction of spin, $\mathbf{p}$ is a unit vector in the direction of the particle momentum with respect to the preferred frame, h is Planck's constant, and K is a constant that characterizes the strength of the LLI violating interaction [3]. This Hamiltonian is manifestly parity violating and produces a dipolar frequency shift which can be measured with high precision. While the authors of Ref. [3] considered only the electron in their discussion, it would appear that the model yields a comparable sensitivity for an interaction with a nuclear spin. We characterize the effective interaction strengths for the electron and nucleus by K_e and K_n, respectively.

The best published limit on K_n is derived from a comparison of the Larmor precession frequencies of ^{199}Hg and ^{201}Hg; the relative frequencies varied by no more than 2.6 μHz in a sidereal day [4]. In most models, the ratio of the intrinsic spin couplings of the Hg isotopes is found to be only 10% different from the ratio of the magnetic moments [5], resulting in experimental limits on a nuclear LLI violating effect of about $K_n < 26$ μHz. The best published limit for electron LLI is from a ferromagnetic torsion pendulum experiment by Phillips [6] which determined $K_e < 2$ mHz. An earlier experiment on the Be^+ ion yielded limits of $K_n < 100$ μHz and $K_e < 0.5$ Hz [7].

Here we describe an experiment which tests LLI by measuring the relative Larmor precession frequencies of Cs and ^{199}Hg as a function of the relative orientation between an applied magnetic field $\mathbf{B}$ and $\mathbf{p}$. The total Hamiltonian (including the magnetic and LLI violating interactions) leads to a net precession frequency $f = |\gamma B + K\hat{\mathbf{B}} \cdot \mathbf{p}|$, where γ is the gyromagnetic ratio ($\gamma_{\mathrm{Cs}} = \gamma_e/4 = 350$ kHz/G and $\gamma_{\mathrm{Hg}} = \gamma_n = 759$ Hz/G). The experiment is sensitive to LLI violating effects due either to the electron (Cs is primarily sensitive to the electron spin) or to the nucleus (Hg has only nuclear spin). The difference between the magnetic field measured by the Cs and ^{199}Hg oscillators can be written as $\Delta B = B_e - B_n = (f_e/\gamma_e - f_n/\gamma_n) - (K_e/\gamma_e - K_n/\gamma_n)\hat{\mathbf{B}} \cdot \mathbf{p}$. By measuring the variation in ΔB with the angle between $\hat{\mathbf{B}}$ and $\mathbf{p}$, we are sensitive only to the terms of interest. Because it is highly unlikely that any LLI violating effects would scale with the gyromagnetic ratios, this approach circumvents the sensitivity suppression that occurred in the earlier comparison of the two Hg isotopes.

A schematic of the basis apparatus is shown in Fig. 1. The optically pumped magnetometer cells are shielded from fluctuations in the ambient magnetic field by a set of three concentric cylindrical molypermalloy shields with end caps. The shield cylinder axis defines the x axis, which we set to point west. Magnetic field coils inside the shields allow the application of highly homogeneous fields in all three directions, and two gradient coils allow the adjustment of gradients in the transverse directions. A stack of three cells is placed at the center of the shields. The cells are stacked along the z axis, which is oriented 45° to the south of vertical in the laboratory. The two outer cells contain Hg vapor and have been constructed similar to those used in a recent Hg electric-dipole moment experiment [8]. The cesium cell has been constructed by fusing glass flats onto the ends of a 1 cm long segment of 31 mm Pyrex tubing. The interior of

0031-9007/95/75(10)/1879(4)$06.00

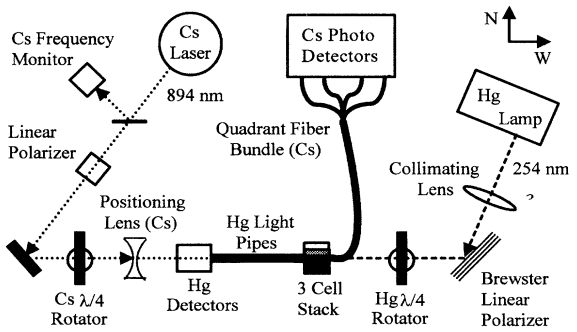

FIG. 1. A schematic showing the essential features of the LLI apparatus. Note that west (W) is along $\hat{\mathbf{i}}$ and north (N) is along $(\hat{\mathbf{j}} - \hat{\mathbf{k}})/\sqrt{2}$. The magnetic shields (around the three cell stack), electronics, and computer are not shown.

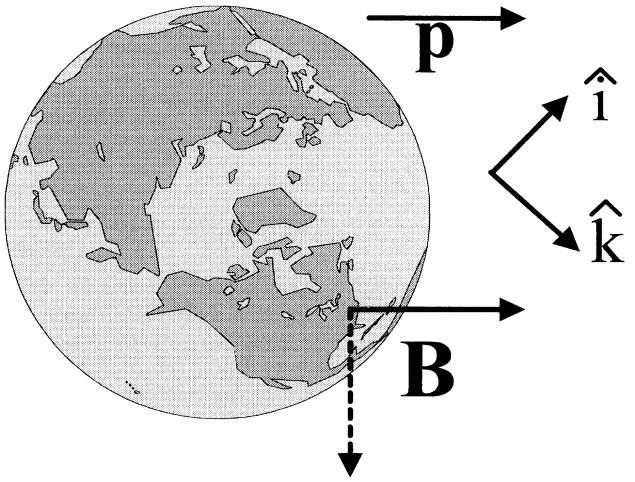

FIG. 2. The experimental geometry looking down from above the Earth's north pole. As the Earth rotates, the relative orientation between the applied magnetic field **B** and the particle momentum, with respect to some preferred frame **p**, varies within a 24 h period. The phase of this oscillation, relative to the Earth's orientation in space, depends on the direction chosen for **B**. The solid line corresponds to $\mathbf{B} = B(-\hat{\mathbf{i}} + \hat{\mathbf{k}})/\sqrt{2}$, while the dashed vector corresponds to $\mathbf{B} = B(\hat{\mathbf{i}} + \hat{\mathbf{k}})/\sqrt{2}$. Data are collected with **B** in each of these directions and their opposites.

the Cs cell is coated with high density paraffin [9], and 65 Torr of neon has been added in order to achieve long spin relaxation times. The Hg and Cs spin relaxation times achieved are typically about 30 s and 30 ms, respectively.

The Hg cells are operated as light absorption oscillators similar to those described in Ref. [4]. The circularly polarized resonant radiation at 254 nm is generated by a ^{204}Hg discharge lamp. The light, propagating along $-x$, illuminates and optically pumps the ^{199}Hg atoms. A static magnetic field is applied parallel to the Earth's equatorial plane along one of four possible directions: $\mathbf{B} = B(\pm\hat{\mathbf{i}} \pm \hat{\mathbf{k}})/\sqrt{2}$, where $B \approx 5.3$ mG, and the signs before the two unit vectors can be independently selected (see Fig. 2). An oscillating magnetic field (oscillating with frequency $f = \omega/2\pi \approx 4.0321$ Hz) is applied along the y axis. When ω is near the Hg Larmor frequency, ω_L, the nuclear spins precess at frequency ω in a cone about **B**. Because the transmission of the circularly polarized light through the sample depends on the spin projection along the x axis, the transmitted light acquires a modulation at ω. The relative phase between the light modulation at ω and B_y is proportional to $\phi = (\omega - \omega_L)\tau$. Thus, if ω remains fixed, the phase change provides a sensitive means of measuring ω_L, and hence B.

While the principles of the Cs and Hg oscillators are similar, the details of the designs are different. The Larmor frequency (ω_L') and hence the corresponding frequency of the oscillating magnetic field (ω') is about $2\pi \times 1.858$ kHz. The 894 nm light required to operate the Cs oscillator is generated by a cavity-stabilized diode laser and propagates in the $+x$ direction. The laser frequency is locked to an external Cs absorption cell that does not contain any buffer gas. The laser cavity has been isolated from variations in room pressure and temperature, regulated so that its cavity length (without locking) varies by less than 2 nm over a 48 h period. This stability is important in that large corrections to the laser cavity length were found to produce small changes in the laser beam intensity profile and thereby create frequency shifts.

Accurate control of the gradients and beam position is crucial, as movement of the Cs beam in the presence of a magnetic gradient across the Cs cell creates an apparent change in the Cs Larmor frequency, even though the static field or gradients do not change. (The Hg cells are far less sensitive to small changes in beam positioning as the longer spin relaxation time allows the Hg atoms to effectively average the field over the entire cell volume.) To enable this control, the laser light transmitted through the Cs oscillator is collected on a quadrant fiber bundle. The intensity of each of the four quadrants is independently monitored, and the Cs beam position is computer controlled by moving a beam steering lens to balance the signals observed in opposing quadrants. By measuring the phase of the signal collected from each quadrant, the gradient dB_z/dx can be effectively measured and minimized before each run.

The signals from the four quadrant detectors are summed, amplified, and sent to a lock-in detector (Stanford Research model SR850). The ultraviolet transmission through the two Hg cells is channeled to solar-blind phototubes by a pair of light pipes constructed of rolled aluminized Mylar. The amplified phototube signals are also sent to SR850 lock-in detectors. So that any drift in reference frequencies will not produce a differential shift between the Cs and Hg phases, the reference frequencies, each set to be very close to the

respective Larmor frequency, are produced by digitally dividing a single 16 MHz clock. To generate the oscillating fields for the Cs and Hg magnetometers, two alternating currents of appropriate amplitude, derived from the synthesized sine waves generated by the Cs and Hg SR850's, respectively, are applied to the B_y field coil. This effectively eliminates many possible sources of electronic phase shift between the oscillators.

The amplitude and phase of each of the lock-in signals is read by a 486 computer through an IEEE interface. Nineteen additional signals are recorded regularly, including the dc levels of all of the four Cs quadrants: the dc intensity transmitted through each cell; the voltages applied to the magnetic field coils; the room temperature, humidity, and pressure; and various laser diagnostics. The computer also controls a variety of experimental parameters including the size of the various correction fields and gradients, the position of the Cs lens (via two micropositioners), and the helicity of the two light beams (via a pair of pneumatic drivers).

An individual data point is collected in the following manner. First, the sensitivity of each of the cells is determined by observing the lock-in response to a well-calibrated change in the homogeneous magnetic field. Following this, the phase of the Cs lock-in detector is used as an error signal which is fed back to B to produce zero phase shift for the Cs oscillator. The magnitude of the effective magnetic field, measured by the Cs cell, is thus held constant (note that the effective magnetic fields may include contributions from light shifts and LLI violating effects). The magnetic gradient dB_z/dz is then adjusted to zero by comparing the effective magnetic field measured by the two Hg oscillators. After these preparatory actions, data collection begins. To account for the shift in the Larmor frequency due to the ac Stark effect (light shifts) of the pumping light, after about 12 min the helicity of the Cs light is reversed (reversing the contributions of the light shift to the Larmor signal) and an additional 12 min of data are collected, followed by reversal of the Hg light helicity. At this point the B feedback is again turned off and the calibration of the cells' sensitivity is repeated, now with the Cs and Hg helicities reversed. The B feedback is then reactivated and data are again taken for 12 min, followed again by reversal of the Cs helicity and a final 12 min of integration. A mean effective magnetic field for each cell is constructed by averaging the normalized effective magnetic field measured in each of the polarizer configurations. Shifts in the effective field associated with optical light shifts ($\approx$70 nG for Hg and 140 nG for Cs) are substantially reduced by this procedure. The difference between the effective mean field measured by the Cs oscillator and the average of the mean effective fields observed by the two Hg oscillators constitutes a measurement of a basic data point. A typical data point is collected approximately every 70 min.

The effective mean field differences over a typical 48 h period contains both an offset and a linear drift. The offset is associated with the finite resolution with which the frequency ratio between the Hg and Cs references can be adjusted, while the drift is probably associated with long term equilibration processes in either the cells or the Hg lamp. A simple linear regression effectively removes both of these effects. The residuals after such regressions, ΔB, have been generated for four 48 h runs taken in each of the four possible orientations of the magnetic field. Figure 3 shows a plot of the measured ΔB vs the time of day, while Fig. 4 shows the same data vs the orientation of **B**. Each of the sets of data is fit (using a Marquardt-Levenberg algorithm) to the function $A\cos(2\pi t/24\text{ h}) + C\sin(2\pi t/24\text{ h})$, where t is in either sidereal or solar hours. The resulting fit parameters for Fig. 3 are $A_D = 171(74)$ pG and $C_D = 46(74)$ pG, suggesting that there may be a slight daily variation in the differential magnetic field measurement. This small variation may be associated with daily fluctuations in the room temperature. Averaging over the four possible orientations of the magnetic field effectively averages away any such daily variations. The fit parameters obtained for the data in Fig. 4, $A_S = -60(74)$ pG and $C_S = -31(74)$ pG, place an upper limit of 0.14 nG on the amplitude of a sinusoidal variation of any phase in the effective differential magnetic field between the cells. This limit corresponds to an upper bound on K_e of about 200 μHz (4 times the limit on the Cs frequency) and on K_n of 110 nHz. These results represent an order-of-magnitude improvement over earlier electron limits and an improvement of a factor of 240 over the previous nuclear limits.

Even in the absence of a violation of LLI it is possible that other effects, coupling the nuclear or electron spins to

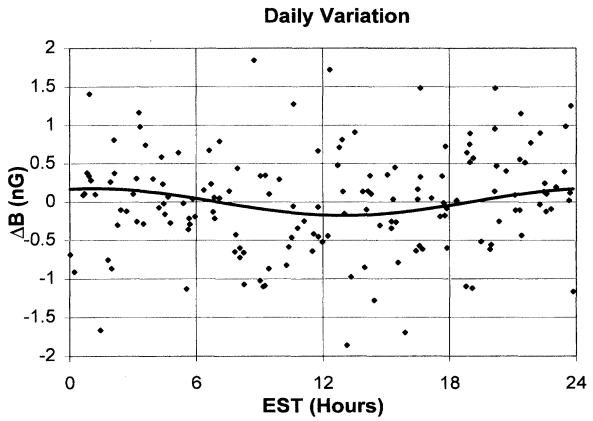

FIG. 3. The difference, ΔB, between the effective magnetic field measured by the cesium and the average of the effective magnetic fields measured by the Hg cells vs the time of day. The solid curve is the best fit sinusoidal curve within a 24 h period.

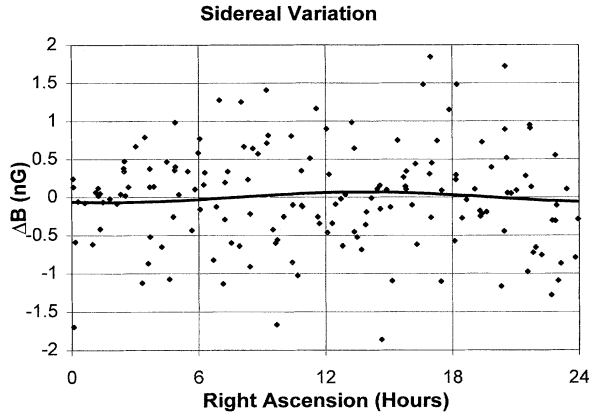

FIG. 4. ΔB as a function of the direction of **B** in space. The solid curve is the best fit sinusoidal curve within a 24 h period.

other particles, could produce a signal in our experiment. An example is the coupling of the spins to the remnant neutrino sea. Following Stodolsky [10], we consider the case where only neutrinos or antineutrinos are present, and that they constitute a degenerate Fermi gas with Fermi level n (measured in electron volts). It is well known from the dipole anisotropy of the remnant blackbody spectra that we are moving at approximately $0.0013c$ toward the Virgo cluster (11.2 h, $-6°$). Stodolsky showed that for this velocity the helicity dependent coherent interaction between electrons and the neutrino sea, due to weak charged currents, would produce an energy splitting between the electron spin states of $8 \times 10^{-28} n^3$ eV. The inclusion of weak neutral currents reduces this prediction by a factor of 2. Neutral currents also produce a shift for the neutron, but reduced by a factor of $g_a/2$, where $g_a = 1.25$ is the weak axial current coupling constant. In a simple shell model where the valence neutron in the ^{199}Hg nucleus is assigned to the $P_{1/2}$ state, there is an additional suppression by a factor of $-1/3$ due to the neutron spin projection [11]. Thus the ^{199}Hg is about 5 times less sensitive than the electron to such an interaction. However, our limits on the Hg nucleus, because of its relatively small (nuclear) magnetic moment, are about 1800 times smaller than those we can place on the electron. Consequently, our best limit on the neutrino Fermi level ($n < 200$ eV) in fact comes from our limit for the Hg nucleus. These limits are not quite as stringent as earlier terrestrial limits ($n < 60$ eV) established from β-decay experiments, and are still a long way from what one might expect from cosmology ($n \approx 7.5 \times 10^{-3}$ eV) [12]. However, unlike the β-decay results, our limit applies to all three species of neutrinos. Because the process is mediated by the weak neutral current, similar limits should apply to remnant supersymmetric neutralinos and all other spin 1/2 dark matter candidates with comparable vector coupling to the Z_0 boson.

In principle, the experimental sensitivity could be improved by several orders of magnitude with a more sophisticated apparatus. The slow (24 h) modulation of the signal allows drifts in the apparatus to dominate the noise. A more rapid modulation of the signal could be achieved by rotating the entire apparatus in a laboratory where the Earth field was substantially reduced. Perhaps even further improvement could be achieved by placing the apparatus on a rapidly rotating spacecraft in a low magnetic field region of space. Any such improvement would likely require the use of superconducting magnetic shielding.

We thank Yulik Khriplovich, Barry Holstein, John Donahue, Kannan Jagannathan, and Tim Chupp for helpful conversations, and Donald Martin, Phillip Grant, Robert Morley, Jessica Smith, Eli Rykoff, and Jared Hertzberg for technical assistance. This work was supported by NSF RUI Grant No. PHY-9402701, a Howard Hughes biomedical research grant, and an Amherst College faculty research award. S. K. L. was supported by NSF Grant No. PHY-9206408.

[1] A. A. Michelson and E. W. Morley, Am. J. Sci. **34**, 333 (1887); Phil. Mag. **24**, 449 (1887).
[2] M. P. Haugan and C. M. Will, Phys. Today **40**, 69 (1987).
[3] H. B. Nielson and I. Picek, Nucl. Phys. **B211**, 269 (1983).
[4] S. K. Lamoreaux, J. P. Jacobs, B. R. Heckel, F. J. Raab, and E. N. Fortson, Phys. Rev. Lett. **57**, 3125 (1986); Phys. Rev. A **39**, 2275 (1987); S. K. Lamoreaux, Phys. Rev. A **42**, 5763 (1990).
[5] E. B. Aleksandrov *et al.*, Sov. Phys. JETP **58**, 1103 (1984).
[6] P. R. Phillips, Phys. Rev. Lett. **59**, 1784 (1987).
[7] J. D. Prestage, J. J. Bollinger, W. M. Itano, and D. J. Wineland, Phys. Rev. Lett. **54**, 2387 (1985).
[8] J. P. Jacobs, W. M. Klipstein, S. K. Lamoreaux, B. R. Heckel, and E. N. Fortson, Phys. Rev. Lett. **71**, 3782 (1993).
[9] V. Liberman and R. J. Knize, Phys. Rev. A **34**, 5115 (1986).
[10] L. Stodolsky, Phys. Rev. Lett. **34**, 110 (1975).
[11] B. J. Venema, P. K. Majumder, S. K. Lamoreaux, B. R. Heckel, and E. N. Fortson, Phys. Rev. Lett. **68**, 135 (1992).
[12] S. Weinberg, *Gravitation and Cosmology* (Wiley, New York, 1972).

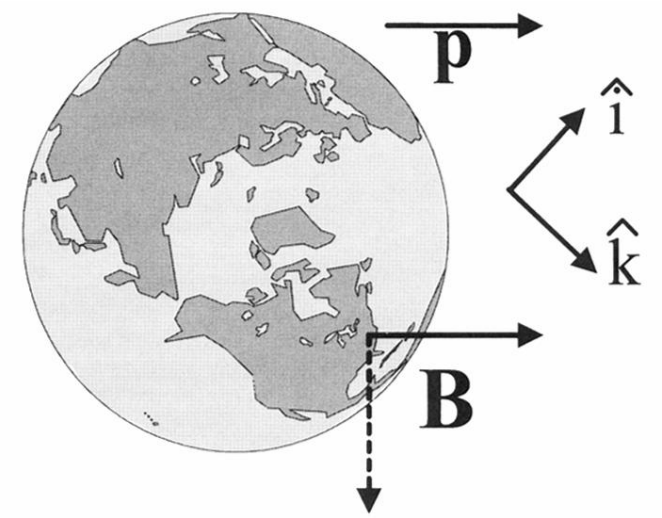

FIG. 2. The experimental geometry looking down from above the Earth's north pole. As the Earth rotates, the relative orientation between the applied magnetic field $\mathbf{B}$ and the particle momentum, with respect to some preferred frame $\mathbf{p}$, varies within a 24 h period. The phase of this oscillation, relative to the Earth's orientation in space, depends on the direction chosen for $\mathbf{B}$. The solid line corresponds to $\mathbf{B} = B(-\hat{\mathbf{i}} + \hat{\mathbf{k}})/\sqrt{2}$, while the dashed vector corresponds to $\mathbf{B} = B(\hat{\mathbf{i}} + \hat{\mathbf{k}})/\sqrt{2}$. Data are collected with $\mathbf{B}$ in each of these directions and their opposites.